Many-electron correlation effects in the generalized oscillator strengths of noble-gas atoms

M. Ya. Amusia,[1,2] L. V. Chernysheva,[2] Z. Felfli,[3] and A. Z. Msezane[3]
[1]*The Racah Institute of Physics, The Hebrew University of Jerusalem, 91904 Jerusalem, Israel*
[2]*A. F. Ioffe Physical-Technical Institute, 194021 St. Petersburg, Russia*
[3]*Center for Theoretical Studies of Physics Systems, Clark Atlanta University, Atlanta, Georgia 30314*
(Received 5 March 2001; published 17 August 2001)

Calculated generalized oscillator strengths for monopole, dipole, and quadrupole discrete and continuous spectrum excitations in Ne, Ar, Kr, and Xe are presented. The results cover the broad range of transferred energy ω, $0 \leqslant \omega < 120$ Ry and momentum q, $0 \leqslant q < 2$ a.u. The calculations were performed in the one-particle Hartree-Fock approximation and with account of many-electron correlations. The latter effects are included via the random phase approximation with exchange, proving to be important in all dipole, monopole, and quadrupole channels as well as in all the domains of the transferred energies and momenta considered. Particularly important are the many-electron correlations at high q values, where new additional purely correlational maxima and minima appear. These results, particularly the maxima and minima are expected to stimulate experimental activity in this domain of atomic physics.

DOI: 10.1103/PhysRevA.64.032711 PACS number(s): 34.50.Fa, 34.80.Dp, 34.10.+x, 31.50.Df

I. INTRODUCTION

Interest in the process of fast-charged particles scattering from complicated structured targets has a long history that goes back to the beginning of the 20th century. Since the early 1920s it had become clear that a fast particle has a small de Broglie wavelength and, consequently, can be used to obtain a type of a x-ray picture of any target, thereby giving information about the internal structure of the target. However, in order to obtain information on the target's structure instead of information on the ''projectile+target'' system, fast projectiles must be used. Otherwise, the interaction between the projectile and target is too strong, causing significant distortions in the target's structure. While the elastic-scattering cross sections are capable of yielding information about the target's initial state, the inelastic scattering can provide information about the dynamics of the process through data that could be called ''dynamical x-ray picture.'' The desire to study this picture stimulated to a large extent the investigation of photoabsorption. However, for frequencies not too high the photoabsorption is dipole. This limits the value of such a picture. On the contrary, the inelastic scattering of fast-charged particles is strongly affected by non-dipole contributions, particularly when the scattering angles are not too small. Therefore, the inelastic scattering process can deliver a much richer ''dynamical x-ray picture'' than obtainable from photoabsorption.

Apart from the purely scientific interest, fast-charged particle inelastic-scattering cross sections for atoms, any finite multiatomic formations and solid bodies are required in a number of other fields of science, such as astrophysics, solid-state physics, and the physics of ionized gases. These data are also of great importance in technological applications, such as, for example, electronics.

The generalized oscillator strength (GOS) concept, introduced by Bethe [1], manifests directly the atomic wave functions and the dynamics of atomic electrons. Apart from converging to the optical oscillator strength (OOS) in the limit of the momentum-transfer squared $q^2 \to 0$ the GOS can provide important information about the electron differential cross sections (DCS's) and the integral cross sections (ICS's) [2]. Lassettre *et al.* [3] established that the GOS approaches the OOS as $q^2 \to 0$ regardless of the electron-impact energy. Following Bethe, the interest in the GOS has been extensive [2–31] for various reasons, particularly: (i) the normalization of measured relative DCS's [8–18]; (ii) the determination of OOS's from absolute DCS's [19–23]; (iii) the calculation of cross sections for energy transfer in molecules [24]; (iv) the evaluation of the singlet-triplet differences [25,26], (v) the calculation of ICS's [27,28], and (vi) the probing of the intricate nature of the valence- and inner-shell electronic excitations [29].

Further interest in the limiting behavior of the GOS as $q^2 \to 0$ has been generated by the difficulty of measuring reliably the electron DCS's for atoms, ions, and molecules at and near zero angle scattering ($\theta = 0°$), [20,32,33]. This difficulty is still clearly manifested even in the most recent measurements of the DCS's [34–38]. The problems of obtaining absolute values of the measured relative electron DCS's using a GOS technique and the contribution to the ICS's from small angular region has been discussed [12]. Recently, various methods have been developed [15,39–41] to guide small-angle electron-scattering measurements. Also, investigations of correlation effects on the GOS minima and maxima have been carried out using the random-phase approximation and exchange (RPAE) [42–45].

Following previous theoretical [46–49] and experimental [49–51] studies, correlation and exchange effects on the characteristic extrema in the GOS for the Ar $3p^6 - 3p^5 4s$ transition were investigated and found to be unimportant [42]. The calculated positions of the extrema [42] have been confirmed by a recent experiment [29] that determined absolute GOS's for various dipole-forbidden and dipole-allowed transitions, including the $2p_{3/2} - 4s$ innershell transition. However, for the resonance transition in Na intershell, correlations were found to influence the characteristic extrema significantly. Furthermore, a previous prediction of strong relativistic effects [52] in the $4p - 5s$ excitation of Kr has

been negated by a recent calculation [45] and measurement [53]. In all the studies above, the GOS was examined as a function of q^2 at a fixed value of the electron-impact energy.

This paper's interest, contrary to all previous studies, is to investigate many-electron correlation effects in the GOS's of the noble gas atoms Ne, Ar, Kr, and Xe, not only their dependence on q but also on the energy transferred, ω. The relatively complicated many-electron systems have been selected to demonstrate that multielectron correlations are very important throughout the domains of ω, $0 \leqslant \omega < 120$ Ry and q, $0 \leqslant q < 2$ Ry studied here. Most previous investigations of the GOS's examined their variation with respect to q only for dipole transitions. Here, monopole and quadrupole transitions are also covered.

II. THEORY OF GENERALIZED OSCILLATOR STRENGTHS

The inelastic scattering cross sections of fast electrons or other charged particles incident upon atoms or molecules are expressed via the GOS $G(\omega,q)$ [1,4] which is a function of the energy ω and the momentum transferred q to the target in the collision process. The GOS is defined as [1] (atomic units are used throughout)

$$G_{fi}(\omega,q)=\frac{2\omega}{q^2}\left|\sum_{j=1}^{N}\int \psi_f^*(\mathbf{r}_1\ldots\mathbf{r}_N)\times\exp(i\mathbf{r}_j\cdot\mathbf{q})\psi_i(\mathbf{r}_1\ldots\mathbf{r}_N)d\mathbf{r}_j\right|^2, \quad (1)$$

where N is the number of atomic electrons and $\psi_{i,f}$ are the atomic wave functions in the initial and final states with energies E_i and E_f, respectively, and $\omega=E_f-E_i$. Because the projectile is assumed to be fast, its wave functions are plane waves and its mass M enters the GOS indirectly, namely, via the energy and momentum-conservation law

$$\frac{p^2}{2M}-\frac{(\mathbf{p}-\mathbf{q})^2}{2M}=\omega. \quad (2)$$

Here, $\mathbf{p}$ is the momentum of the projectile. It follows from the GOS definition Eq. (1) that when $q=0$, the GOS coincides with the OOS or is simply proportional to the photoionization cross section (see for example [4,35]), depending upon whether the final state is a discrete excitation or belongs to the continuous spectrum. The energy ω enters the GOS directly via a factor in Eq. (1), and indirectly, via the energy E_f of the final state $|f\rangle$.

In the one-electron Hartree-Fock approximation (HF) Eq. (1) simplifies considerably, reducing to the following expression:

$$g_{fi}(\omega,q)=\frac{2\omega}{q^2}\left|\sum_{n_i,k_f}\int \phi_{k_f}^*(\mathbf{r})\exp(i\mathbf{q}\cdot\mathbf{r})\phi_{n_i}(\mathbf{r})d\mathbf{r}\right|^2, \quad (3)$$

where ϕ_{n_i,k_f} are the Hartree-Fock wave functions. The summation is performed over all one electron initial n_i and final k_f states that satisfy the energy conservation relation Eq. (2) and have the same spin. The transition operator $\hat{A}(q) \equiv \exp(i\mathbf{q}\cdot\mathbf{r})$ can be represented as a sum of contributions with different multipolarities $\hat{A}_l(q)$ of which we retain the largest ones, namely, the dipole $l=1$, monopole $l=0$, and quadrupole $l=2$ terms. Then the GOS amplitudes, which are matrix elements of $\hat{A}_l(q)$, are obtained by performing numerical integration of $\hat{A}_l(q)$ and a product of the two HF wave functions.

The next step in the GOS calculation is to take into account the many-electron correlations. This can be done only approximately due to the very complicated nature of the precise wave functions $\psi_{i,f}(\mathbf{r}_1\ldots\mathbf{r}_N)$. In this paper, we take into account the many-electron correlations within the framework of the random-phase approximation with exchange (RPAE) [54,55]. This approximation has been applied very successfully to photoionization studies [54]. It is also capable of describing experimental data in this field, e.g., data on photon absorption by iodine [56], nondipole corrections to the photoelectron angular distributions in noble gases [57,58], as well as extrema in atomic GOS's [42–45].

In order to obtain the matrix elements of the transition operator $\hat{A}_{RPAE}(\omega,q)$ in the RPAE framework, an integral equation has been solved. This equation can be represented symbolically as [55]

$$\hat{A}_{RPAE}(\omega,q)=\hat{A}(q)+\hat{A}_{RPAE}(\omega,q)\times\hat{\chi}(\omega)\times\hat{U}. \quad (4)$$

Here, $\hat{\chi}(\omega)\equiv(\omega-\hat{H}_{ev})^{-1}-(\omega+\hat{H}_{ev})^{-1}$ describes the propagation of noninteracting virtually created electron-vacancy pair with the Hamiltonian $\hat{H}_{ev}$; $\hat{U}$ denotes the combination of direct and exchange terms of the interelectron Coulomb potential $V_{12}=1/|\vec{r}_1-\vec{r}_2|$. Equation (4) can be solved, also symbolically, leading to the expression

$$\hat{A}_{RPAE}(\omega,q)=\frac{\hat{A}_q}{\hat{1}-\hat{\chi}(\omega)\times\hat{U}}. \quad (5)$$

This equation permits the qualitative investigation of the general features of collective multi-electron effects in the GOS's. Indeed, we are looking for their strong enhancement that corresponds to zero denominator in Eq. (5). The frequencies Ω that are solutions of the equation

$$\hat{1}-\hat{\chi}(\Omega)\times\hat{U}=0 \quad (6)$$

are called giant resonances (GR's).

Multielectron correlations can manifest themselves also in interference resonances (IR's) and correlation minima (CM). In IR's, the transition operator of, for example, an outer atomic shell $\hat{A}^{(o)}_{RPAE}(\omega_{IR},q)$ is much greater than $\hat{A}^{(o)}(q)$. This occurs because of the large transition operator $\hat{A}^{(i)}_{RPAE}(\omega_{IR},q)$ from the inner subshell, which is strongly coupled to that from the outer shell by the intershell interaction $\hat{U}^{(io)}$, so that

$$\hat{A}^{(o)}_{RPAE}(\omega_{IR},q)\approx\hat{A}^{(i)}_{RPAE}(\omega_{IR},q)\times\chi^{(i)}(\omega)\times\hat{U}^{(io)}\gg\hat{A}^{(o)}(q). \tag{7}$$

At the correlation minima, destructive interference occurs, so that $\hat{A}_{RPAE}(\omega_{CM},q)=0$, while $\hat{A}^{(o)}(q)\neq 0$.

Nonsymbolically, Eq. (4) is usually presented in matrix form, which naturally, looks much more complicated than Eq. (4):

$$\langle f|\hat{A}_{RPAE}(\omega,q)|i\rangle=\langle f|\exp(i\mathbf{q}\cdot\mathbf{r})|i\rangle + \left(\sum_{n'\leqslant F,k'>F}-\sum_{n'>F,k'<F}\right) \times\frac{\langle k'|\hat{A}_{RPAE}(\omega,q)|n'\rangle\langle n'f|U|k'i\rangle}{\omega-\varepsilon_{k'}+\varepsilon_{n'}+i\,\eta(1-2n_{k'})}. \tag{8}$$

Here, $\leqslant F$ $(>F)$ denotes occupied (vacant) HF states, ε_n are the one electron HF energies, $\eta\to 0$, and $n_k=1(0)$ for $k\leqslant F$ $(>F)$; $\langle nf|U|ki\rangle\equiv\langle nf|V|ki\rangle-\langle nf|V|ik\rangle$. The procedure of its solution is described in details [54,55]. Note that contrary to $\hat{A}(q)$, $\hat{A}_{RPAE}(\omega,q)$ is a nonlocal operator, which corresponds to two space coordinates $\mathbf{r}$ and $\mathbf{r}'$ instead of only one $\mathbf{r}$ in $\hat{A}(q)$.

Using Eq. (4), one can represent the GOS's with an account of many-electron RPAE correlations in the following form:

$$G^{RPAE}_{fi}(\omega,q)=\frac{2\omega}{q^2}|\langle f|\hat{A}_{RPAE}(\omega,q)|i\rangle|^2. \tag{9}$$

Here, $\langle f|$ and $|i\rangle$ are, respectively, the final and initial HF states. Eqs. (4) and (8) for $\hat{A}_{RPAE}(\omega,q)$ decouple into a system of independent equations for partial contributions with a given angular momentum l, $\hat{A}^{l}_{RPAE}(\omega,q)$, which we solved numerically, as it is described in [55]. The operator of the interaction between fast charged particles and atomic electrons can be represented in another form than $\hat{A}(q)=\hat{A}^{r}(q)\equiv\exp(i\mathbf{q}\cdot\mathbf{r})$. This is analogous to the case of photoionization and can be called *length* form. The other one is similar to the *velocity* form in photoionization and looks like [55]

$$\hat{A}^{v}(\omega,q)=[\exp(i\mathbf{q}\cdot\mathbf{r})(\mathbf{q}\cdot\boldsymbol{\nabla}-\mathbf{q}\cdot\vec{\boldsymbol{\nabla}})\exp(i\mathbf{q}\cdot\mathbf{r})], \tag{10}$$

where the upper arrow in $\vec{\boldsymbol{\nabla}}$ in Eq. (10) implies that the function standing to the left is being operated on.

III. RESULTS OF CALCULATIONS

As has already been mentioned in the introduction, the main aim of this paper is to present results of extensive calculations of the GOS's of noble-gas atoms Ne, Ar, Kr, and Xe. The calculations are performed in a very broad region of the energy transferred to the atom ω (up to 120 Ry) and momentum q (up to 2 atomic units). The results are obtained in the one electron HF approximation and with an account of multielectron correlations within the RPAE. Three multipoles were considered in the calculations of the GOS's; they correspond to the dipole, monopole, and quadrupole transitions. We want to demonstrate the variation of the role of correlation effects with the growth of ω and q.

The ω dependence of the dipole GOS's for $q\to 0$ is reasonably well known because, for $q=0$, the GOS's are simply proportional to the extensively studied photoionization cross sections. Extremely strong multielectron effects were found there in a very broad photon frequency range, from the outer shells to well above the inner-shell thresholds. It is known that the whole variety of correlation effects, namely the intra- and inter-shell interaction proved to be very important in photoionization. Most prominent among these effects are the dipole giant and correlation resonances [54]. However, almost nothing is known about the variation of these resonances in GOS's with the growth of q even in the dipole channel. The monopole and quadrupole GOS's have never been studied from this point of view at all.

In this paper, GOS's for outer and intermediate subshell electrons have been calculated, namely, for the following subshells: $2p^6$, $2s^2$, $1s^2$ in Ne, $3p^6$, $3s^2$ in Ar, $4p^6$, $4s^2$ and $3d^{10}$ in Kr, $5p^6$, $5s^2$, and $4d^{10}$ in Xe. The interaction among all these electrons has been taken into account while solving Eq. (8). In order to check the numerical accuracy of our calculations, the latter were performed in two forms of the transition operator $\hat{A}(q)$, namely, the length form $\hat{A}^{r}(q)$ and the velocity form $\hat{A}^{v}(q)$. In RPAE, just as in calculations with precise wave functions, the results in these two forms must agree. An agreement within a 1–2% error between the two forms was considered as acceptable in all our calculations. Consequently, here we present only the length form of our results.

The results demonstrate an unexpected richness of the interelectron interaction effects, which persist with the increase of the energy ω and momentum q for all the GOS's considered: monopole, dipole, and quadrupole, in all atoms. The multielectron effects in Kr and especially in Xe, are particularly strong. With the growth of q, the giant and correlation resonances are strongly modified. Apart from them, with an increase of q, new maxima also appear for all, i.e., dipole, monopole, and quadrupole GOS's. The interelectron interaction dramatically affects the GOS's of the few-electron subvalent subshells ns^2. At high ω, these subshells affect considerably the GOS's of neighboring multielectron shells.

In our investigation of correlation effects on the GOS's of monopole, dipole, and quadrupole transitions of Ne, Ar, Kr, and Xe, we generated many HF and RPAE GOS densities and ratios of the latter to the former. To keep the manuscript within a reasonable length and convey succinctly the most important results of our consideration, we have carefully selected a number of representative figures to be displayed here. We also refer in the description of results to other data not displayed, but that can be obtained directly from the authors. The essentials of our objectives are, nevertheless captured in the many representative figures presented below.

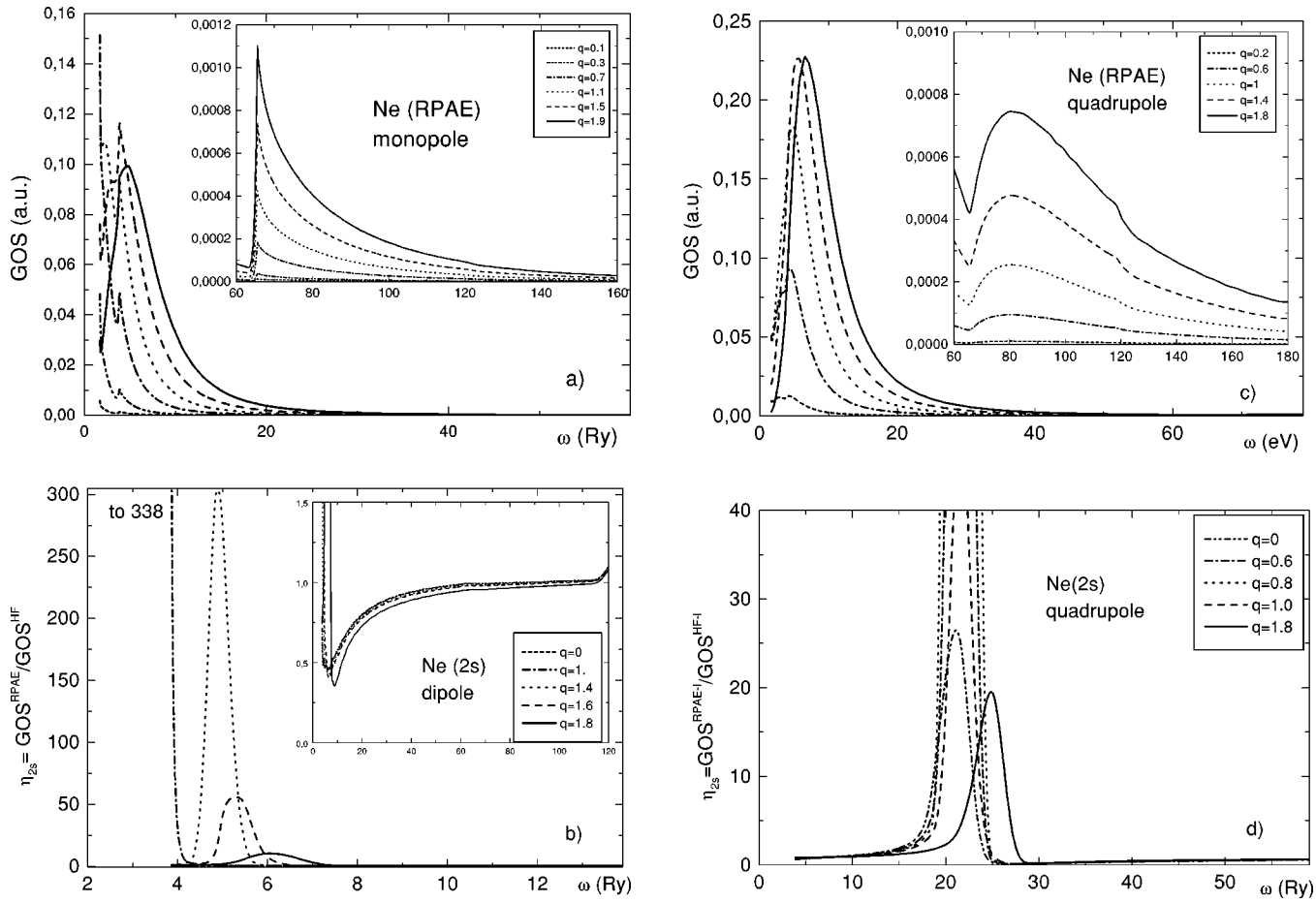

FIG. 1. Generalized Oscillator Strengths for Ne atom as functions of the transferred energy ω (Ry) and momentum q (a.u). (a) *Monopole* GOS total density $[G^{RPAE}_{2p\to\varepsilon p}(\omega,q)+G^{RPAE}_{2s\to\varepsilon s}(\omega,q)]$ in RPAE. (b) Ratio of *dipole* GOS densities for *2s* electrons, with and without RPAE correlations, $\eta_{2s\to\varepsilon p}(\omega,q)\equiv G^{RPAE}_{2s\to\varepsilon p}(\omega,q)/G^{HF}_{2s\to\varepsilon p}(\omega,q)$. (c) Quadrupole GOS total density $[G^{RPAE}_{2s\to\varepsilon d}(\omega,q)+G^{RPAE}_{2p\to\varepsilon f,p}(\omega,q)]$ in RPAE. (d) Ratio of *quadrupole* GOS densities for *2s* electrons, with and without RPAE correlations, $\eta_{2s\to\varepsilon d}(\omega,q)$.

A. Calculated results for the Ne atom

1. Ne monopole channel

Figure 1(a) demonstrates the behavior of the monopole GOS total densities $[G^{RPAE}_{2p\to\epsilon p}(\omega,q)+G^{RPAE}_{2s\to\epsilon s}(\omega,q)]$ in the RPAE as both q and ω vary from 0.1 to 1.9 a.u. and I (I being the ionization potential) through 160 Ry, respectively. As seen in this channel, the GOS's, characterized by two sets of maxima, are rapidly increasing with the growth of q. A prominent maximum, a kind of shape resonance, appears as early as when $q=0.1$ a.u. at $\omega_{\max}\cong 3.8$ Ry and moves to $\omega_{\max}\cong 4.8$ Ry when $q=1.9$ a.u. The magnitude of this maximum increases dramatically when q increases from 0.1 to 1.9 a.u., but reaching its peak at $q=1.5$ a.u. before it starts to decrease. The insert shows the variation of the GOS densities over the range $60\leqslant\omega\leqslant 160$ Ry. A second set of maxima appears that increase monotonically with q and whose magnitudes are much smaller than those of the first set. Their position is at $\omega_{\max}\cong 65$ Ry and is independent of q. The RPAE correlations are essential for the $2p\to\epsilon p$ transition, but they are also noticeable for the $2s\to\epsilon s$ transition (results not shown).

2. Ne dipole channel

In the dipole channel, the GOS's are decreasing with increasing q, consistent with the general expressions Eqs. (1), (3), and (9). Correlations affect the transition considerably for all values of q and ω considered. The ratio $\eta_{2p\to\epsilon d,s}(\omega,q)\equiv G^{RPAE}_{2p\to\epsilon d,s}(\omega,q)/G^{HF}_{2p\to\epsilon d,s}(\omega)$ varies from 0.4 to 1.2 over the range of ω values. As an example, Fig. 1(b) illustrates the variation with q and ω of the ratio $\eta_{2s\to\epsilon p}(\omega,q)\equiv G^{RPAE}_{2s\to\epsilon p}(\omega,q)/G^{HF}_{2s\to\epsilon p}(\omega)$ for the dipole channel of the Ne $2s$ electrons. Clearly, for the $G^{RPAE}_{2s\to\epsilon p}(\omega,q)$ the role of correlations is much stronger near threshold and becomes insignificant as ω increases beyond about 20 Ry. Indeed, this ratio $\eta_{2s\to\epsilon p}(\omega,q)$ grows with q and reaches the value of about 11.7 when $q=1.8$ a.u. This manifests the presence of correlation maxima and interference resonances [see Eq. (7)] in the $2s\to\epsilon p$ transition.

3. Ne quadrupole channel

Just as in the monopole transition, the RPAE GOS's for the Ne quadrupole channel increase rapidly with the growth of q from 0.2 through 1.8 a.u. as shown in Fig. 1(c). Here, too the transition is characterized by two sets of maxima, the

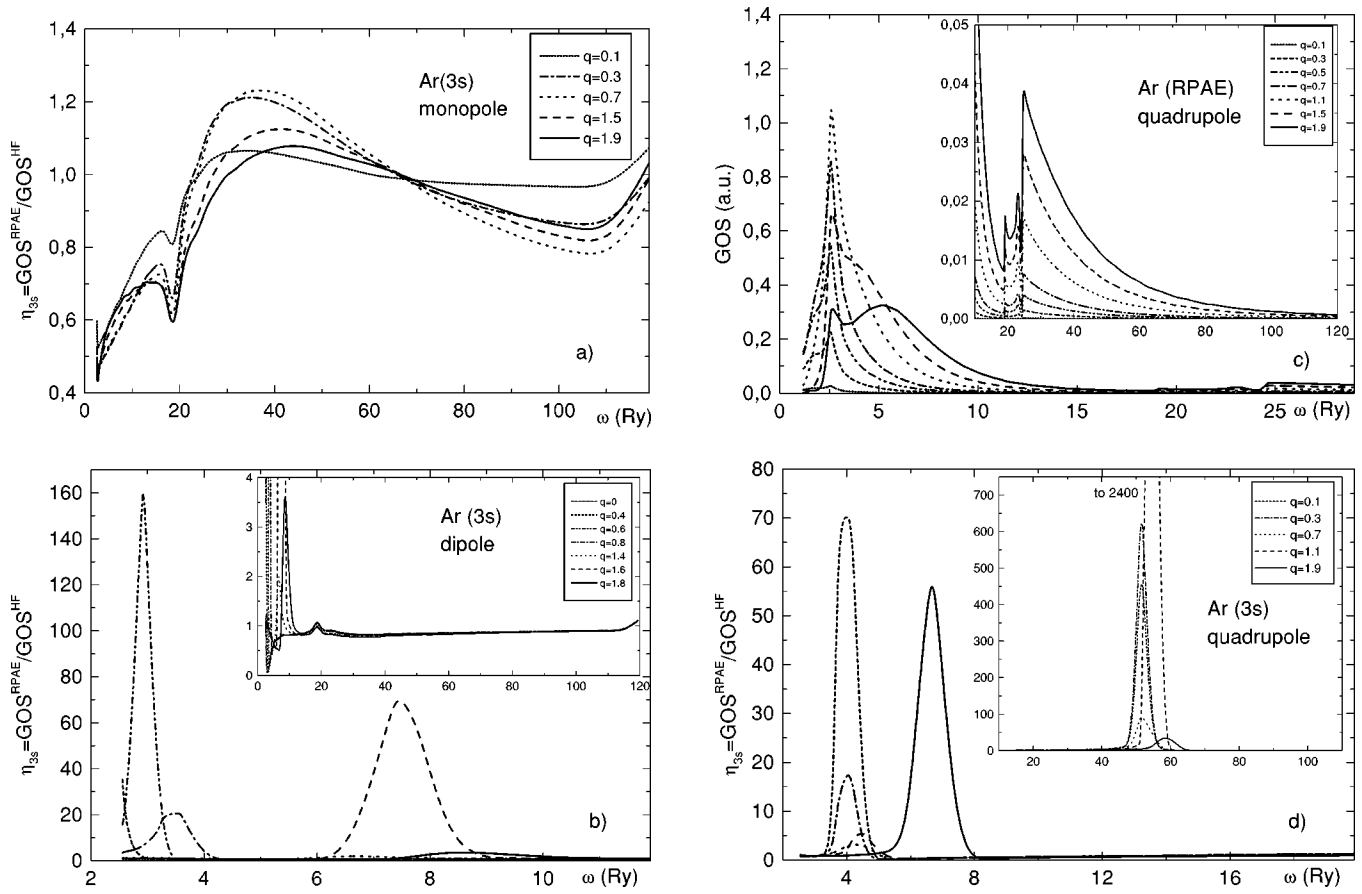

FIG. 2. Generalized Oscillator Strengths for Ar atom as functions of the transferred energy ω (Ry) and momentum q (a.u). (a) Ratio of *monopole* GOS densities for *3s* electrons, with and without RPAE correlations, $\eta_{3s\to\varepsilon p}(\omega,q)\equiv G^{RPAE}_{3s\to\varepsilon p}(\omega,q)/G^{HF}_{3s\to\varepsilon p}(\omega,q)$. (b) Ratio of *dipole* GOS densities for *3s* electrons, with and without RPAE correlations, $\eta_{3s\to\varepsilon p}(\omega,q)$. (c) *Quadrupole* GOS total density $[G^{RPAE}_{3p\to\varepsilon f,p}(\omega,q)+G^{RPAE}_{3s\to\varepsilon d}(\omega,q)]$ in RPAE. (d) Ratio of quadrupole GOS densities for Ar 3s electrons, with and without RPAE correlations.

first maximum of the first set occurs at $\omega_{\max}\cong 4.3$ Ry and the last at $\omega_{\max}\cong 6.6$ Ry, corresponding to values of $q=0.2$ and 1.8 a.u., respectively. This maximum increases rapidly from a near zero value for $q=0.2$ a.u. to about 0.23 for $q=1.4$ through 1.6 a.u. The position of the second set of maxima at about $\omega_{\max}\cong 80$ Ry is independent of q, but their magnitudes increase monotonically with q as it grows from 0.2 to 1.8 a.u.

For the Ne quadrupole transition, the correlations, determined by the ratio $\eta_{2p\to\epsilon f,p}(\omega,q)$, are important as q increases; they vary from 0.8 to 1.4. Much more important, however, are the corrections in the $2s\to\epsilon d$ transition. The corresponding ratio $\eta_{2s\to\epsilon d}(\omega,q)=G^{RPAE}_{2s\to\epsilon d}(\omega,q)/G^{HF}_{2s\to\epsilon d}(\omega,q)$, shown in Fig. 1(d) increases dramatically, by more than a factor of 200 in the narrow range $23\leqslant\omega\leqslant 25$ Ry, for q varying from 0 through 1.8 a.u., then decrease to a value of about 27 at $q=1.8$ a.u. Beyond about 30 Ry correlations remain insignificant all the way through 120 Ry.

B. Calculated results for the Ar atom

1. Ar monopole channel

In the monopole channel of the Ar atom, the GOS's initially increase rapidly with q, then reach an absolute maximum when $q\cong 1.1$ a.u. of magnitude of about 0.25 before they begin decreasing. The position of the first maximum of the first set of maxima occurs at $\omega_{\max}\cong 2.7$ Ry and corresponds to $q=1.1$ a.u. It moves to higher values of ω with increase in q, reaching the value of about 0.1 when $\omega_{\max}\cong 5$ Ry. Two other sets of maxima, about an order of magnitude smaller than the first set, occur at $\omega_{\max}\cong 20$ Ry and $\omega_{\max}\cong 25$ Ry, with their positions independent of q but their magnitudes being reversed in comparison with the first set. The maximum corresponding to $q=1.9$ a.u. dominates, followed by those belonging to $q=1.5$, 1.1 a.u., etc., in both sets.

The monopole GOS's of the inner subshells $2p^6$ and $2s^2$ grow rapidly as ω increases. The ratio $\eta_{3p\to\epsilon p}(\omega,q)$ differs considerably from unity, demonstrating the significance of correlation effects for this transition (figure also not shown). Much more important, however, are the correlations in the monopole $3s\to\epsilon s$ transition, manifested through $\eta_{3s\to\epsilon s}(\omega,q)$ which varies between about 0.4 and 1.2 and has an interesting dependence on both ω and q as shown in Fig. 2(a). This ratio is characterized by essentially two sets of broad maxima for a fixed value of q, while ω varies from the ionization threshold to about 120 Ry. Interestingly, for $q=0.1$ a.u. correlations diminish considerably as

$\omega \rightarrow 120$ Ry, while their significance persists for the remainder of the q values.

2. Ar dipole channel

Just as in Ne, the Ar dipole channel GOS's are increasing with ω for all the values of q varying from 0 through 1.8 a.u. The position of the maximum associated with the $3p$ ionization threshold, while the maximum itself is decreasing in magnitude, moves to higher energies, from $\omega_{\max} \cong 1.5$ Ry at $q=0$ to $\omega_{\max} \cong 3$ Ry at $q=1.8$ a.u. Two additional maxima appear at $\omega_{\max} \cong 20$ Ry and $\omega_{\max} \cong 25$ Ry, whose positions are independent of the values of q, but their magnitudes are roughly an order of magnitude smaller than the first maximum corresponding to $q=0$. Correlations are large for the $3p \rightarrow \epsilon d,s$ transitions, so that the ratio $\eta_{3s \rightarrow \epsilon d,s}(\omega,q)$ varies between 0.25 and 1.9 within the range $0 \leqslant \omega \leqslant 23$ Ry. As an illustration of the importance of correlations on the GOS's for the Ar dipole channel, Fig. 2(b) presents calculated results for the $\eta_{3s \rightarrow \epsilon p}(\omega,q)$. Clearly, the great importance of correlations in this transition is evident. They are a manifestation of the presence of the Interference Resonance in the $3s$ subshell photoionization (see, for example, Ref. [54]). We note, that their significance diminishes considerably beyond about $\omega=30$ Ry.

3. Ar quadrupole channel

The quadrupole channel GOS's for Ar, displayed in Fig. 2(c) increase rapidly with q as it moves from 0.5 a.u. through 1.9 a.u. Here, the structure of the GOS curves is more complicated than that for the monopole transition. The associated first set of maxima, with their positions almost fixed with respect to q variation at $\omega_{\max} \cong 2.5$ Ry, peak at $q=1.1$ a.u. before they begin to decrease as q increases beyond $q=1.1$ a.u. through 1.9 a.u. There are three additional sets of maxima at $\omega_{\max} \cong 20$, 24, and 25 Ry. For each of the three sets of maxima, contrary to the first set, the order of significance of the maxima is reversed, viz. the $q=1.9$ a.u. curve has become the most dominant, followed by those at $q=1.5$, 1.1 a.u., down to $q=0.1$ a.u.

The ratio $\eta_{3p \rightarrow \epsilon f,p}(\omega,q)$ varies from 0.8 to 1.6 within the range $0 \leqslant \omega \leqslant 30$ Ry. However, most interesting is the behavior of the ratio $\eta_{3s \rightarrow \epsilon d}(\omega,q)$ as a function of ω displayed in Fig. 2(d). It is characterized by two sets of relatively narrow, sharp, and large maxima. In the first set, the maximum moves from $\omega_{\max} \cong 4.1$ Ry at $q=0.1$ a.u. through $\omega_{\max} \cong 4.4$ Ry at $q=0.7$ a.u. to $\omega_{\max} \cong 6.7$ Ry at $q=1.9$ a.u. and decreases from 70 to 4 and then increases up to 58. In the second set, the maximum is much larger with $\eta_{3s \rightarrow \epsilon d}(\omega,q) = 312$ at $\omega_{\max} \cong 51.8$ Ry for the $q=0.1$ a.u. curve and decreasing to $\eta_{3s \rightarrow \epsilon d}(\omega,q)=34.6$ at $\omega_{\max} \cong 58.8$ Ry for the $q=1.9$ a.u. curve.

C. Calculated Values for the Kr atom

1. Kr monopole channel

For the monopole channel, the GOS's of Kr behave similarly to those of Ar. The GOS's begin by rapidly increasing with q up to $q=0.7$ a.u., then they rapidly decrease when q increases from 1.1 a.u. through 1.9 a.u. The first set of maxima reach absolute maximum value at $q=1.1$ a.u. when $\omega_{\max} \cong 2.5$ Ry, then begin to decrease as q approaches 1.9 a.u. The corresponding position of the maximum moves toward higher energies, from $\omega_{\max} \cong 2.3$ Ry at $q=0.1$ a.u. to $\omega_{\max} \cong 5.35$ Ry at $q=1.9$ a.u. The dependence of the monopole GOS's upon ω and q is illustrated in Fig. 3(a). Here, also, a second set of maxima, independent of q, appears at about $\omega_{\max} \cong 7.5$ Ry. The magnitudes of these maxima increase with increase of q, with the largest value corresponding to $q=1.9$ a.u. and the lowest to $q=0.1$ a.u.

The ratio $\eta_{4p \rightarrow \epsilon p}(\omega,q)$ for the $4p \rightarrow \epsilon p$ transition is affected considerably by RPAE correlations, varying from 0.2 to 1.3 for $0 \leqslant \omega < 30$ Ry. Then this ratio approaches unity as the energy increases toward 120 Ry. The ratio $\eta_{4s \rightarrow \epsilon s}(\omega,q)$ for the $4s \rightarrow \epsilon s$ transition is affected by RPAE correlations much stronger than that for $4p \rightarrow \epsilon p$ transition, varying from 0.45 to 1.55 for $0 \leqslant \omega < 70$ Ry. Consequently, the ratio $\eta_{4s \rightarrow \epsilon s}(\omega,q)$ approaches unity at considerably higher energies than the $\eta_{4p \rightarrow \epsilon p}(\omega,q)$ ratio. RPAE correlations influence the GOS's for the $3d \rightarrow \epsilon d$ transition even over a broader energy range. This ratio is illustrated in Fig. 3(b), where it is seen that $\eta_{3d \rightarrow \epsilon d}(\omega,q)$ deviates significantly from unity over the entire energy domain, $I_{3d} < \omega < 120$ Ry, where I_{3d} is the ionization potential of the $3d$ subshell.

2. Kr dipole channel

Figure 3(c) depicts the variation of the dipole GOS's in Kr as a function of both q and ω. Just as in the cases of Ne and Ar, the dipole GOS's are characterized by two sets of maxima. The positions of the maxima near the ionization threshold move forward from 1.3 to 4 Ry when q varies from 0.1 a.u. through 1.9 a.u. and the magnitudes of the maxima decrease from about 6 to 0.4 with the increase of q from 0.1 a.u. through 1.9 a.u. A second set of maxima, much broader than the first set for a given q value, appears in the range $15 \leqslant \omega \leqslant 20$ Ry. Contrary to the Ar quadrupole channel and Kr monopole channel, the magnitudes of the maxima in the first and second sets maintain the same order and decrease with increase in q, viz. the largest magnitude of the maxima corresponds to $q=0.1$ a.u. and the lowest to $q=1.9$ a.u.

The interesting variation from about 0.4 to 2.0 of the ratio $\eta_{4p \rightarrow \epsilon d,s}(\omega,q)$ for $I_{4p} < \omega \leqslant 30$ Ry where I_{4p} is the ionization potential of the $4p$ subshell, is displayed in Fig. 3(d). The variation of this ratio with ω, manifests its strong influence by the multi-electron correlations, namely the giant resonance in the $3d \rightarrow \epsilon f$ transition. Beyond about 30 Ry the influence of correlations is unimportant as both ω and q vary. The magnitudes of the maxima decrease with increase in q and their positions move forward as q moves from 0.1 to 1.9 a.u. The behavior is similar to that for the Kr dipole GOS's of Fig. 3(c). The variation of $\eta_{4s \rightarrow \epsilon p}(\omega,q)$ within a relatively narrow energy range is even stronger than that of the $\eta_{4p \rightarrow \epsilon d,s}(\omega,q)$. The ratio $\eta_{3d \rightarrow \epsilon f,p}(\omega,q)$ deviates slightly from unity, varying between 0.8 and 1.1 over the entire range of ω. This demonstrates a mild influence of correlation effects on the $3d \rightarrow \epsilon f,p$ transition.

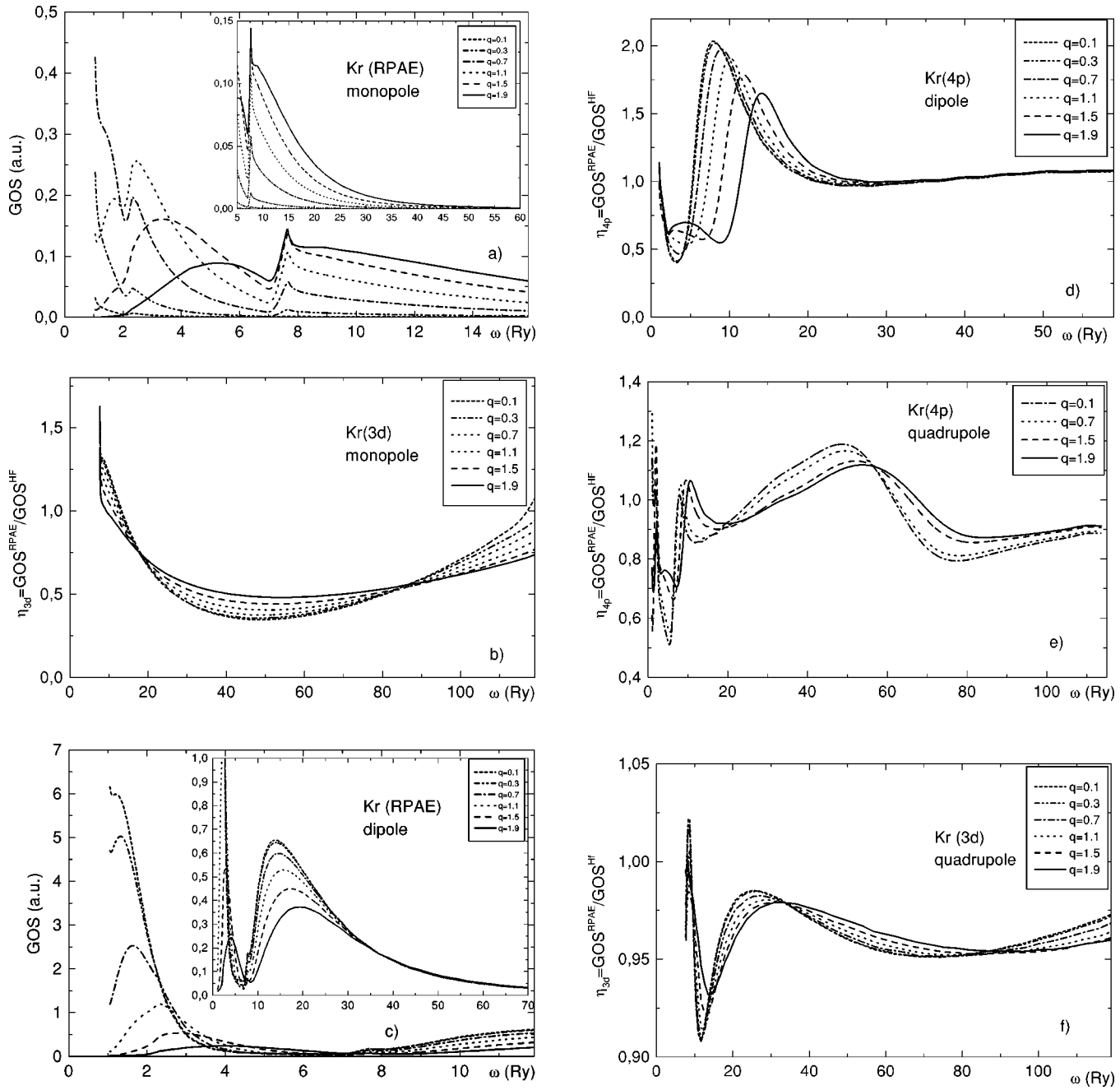

FIG. 3. Generalized Oscillator Strengths for Kr atom as functions of the transferred energy ω (Ry) and momentum q (a.u). (a) *Monopole* GOS total density $[G^{RPAE}_{4p\to\varepsilon p}(\omega,q)+G^{RPAE}_{4s\to\varepsilon s}(\omega,q)+G^{RPAE}_{3d\to\varepsilon d}(\omega,q)]$ in RPAE. (b) Ratio of *monopole* GOS densities for *3d* electrons, with and without RPAE correlations, $\eta_{3d\to\varepsilon d}(\omega,q)\equiv G^{RPAE}_{3d\to\varepsilon d}(\omega,q)/G^{HF}_{3d\to\varepsilon d}(\omega,q)$. (c) *Dipole* GOS total density $[G^{RPAE}_{4p\to\varepsilon d,s}(\omega,q)+G^{RPAE}_{4s\to\varepsilon p}(\omega,q)+G^{RPAE}_{3d\to\varepsilon f,p}(\omega,q)]$ in RPAE. (d) Ratio of *dipole* GOS densities for *4p* electrons, with and without RPAE correlations, $\eta_{4p\to\varepsilon d,s}(\omega,q)\equiv G^{RPAE}_{4p\to\varepsilon d,s}(\omega,q)/G^{HF}_{4p\to\varepsilon d,s}(\omega,q)$. (e) Ratio of *quadrupole* GOS densities for *4p* electrons, with and without RPAE correlations, $\eta_{4p\to\varepsilon f,p}(\omega,q)$. (f) Ratio of *quadrupole* GOS densities for *3d* electrons, with and without RPAE correlations, $\eta_{3d\to\varepsilon g,s}(\omega,q)$.

3. Kr quadrupole channel

The quadrupole GOS's in Kr are characterized by two sets of prominent maxima. The first set of maxima increases with q as it varies from 0.1 to 1.1 a.u., where the maxima reach their absolute maximum value, before they decrease with increasing q. As q varies from 0.1 to 1.9 a.u. The corresponding positions of the first set of maxima move from 2.3 to 4.3 Ry. The second set of maxima increases with q, including their positions, but only slightly; when $q=0.3$ a.u., $\omega_{\max}\cong 13.8$ Ry and when $q=1.9$ a.u., $\omega_{\max}\cong 20$ Ry. This behavior is similar to that for Ne and Ar transitions.

Figure 3(e) presents the variation of the ratio $\eta_{4p\to\epsilon f,p}(\omega,q)$ with ω and q. Clearly, it is rather a complicated oscillatory function of both ω and q for all the values of q considered, from 0.1 through 1.9 a.u. This behavior manifests the significance of correlation effects for this ratio.

We note that here the positions of the maxima shift to higher values of ω as q increases from 0.1 through 1.9 a.u. The ratio $\eta_{4s\to\epsilon d}(\omega,q)$ (not shown) reaches extremely large values, as much as 2000 for small q, $q=0.14$ a.u. and $\omega<10$ Ry. The RPAE correlations in the quadrupole GOS's of the $3d$ subshell in Kr are quite small, but are represented by a smooth oscillating curve, given in Fig. 3(f). As in the previous figure, the positions of the maxima are shifted forward to large values of ω as q increases from 0.1 through 1.9 a.u.

D. Calculated values for Xe atom

1. Xe monopole channel

The monopole GOS's in Xe, just as in the other noble gases, increase rapidly near the ionization threshold, I_{5p} with increase of q and reach their largest value at $q=0.7$ a.u. Here, also, the GOS's are characterized by two sets of maxima. For the first set, a maximum appears for $q=1.1$ a.u. and disappears by $q=1.9$ a.u. while decreasing in magnitude. A second set of maxima appears at about 6 Ry. The maximum being very small for $q=0.1$ a.u., increases rapidly with q and reaches its absolute maximum value at $q=1.5$ a.u., whose magnitude is almost as large as the one at $q=1.1$ a.u. Interestingly, here the effect of the large Z of Xe is clearly manifest, particularly on the second set of the maxima: they are pulled strongly closer to I_{5p} in comparison with those of Ne, Ar, and Kr.

Figure 4(a) shows the variation of the ratio $\eta_{5p\to\epsilon p}(\omega,q)$ for the $5p\to\epsilon p$ transition in Xe. It is affected by RPAE correlations much stronger than that for the $4p\to\epsilon p$ transition in Kr, varying from 0.2 to 5 for $I_{5p}<w<10$ Ry. For ω greater than about 30 Ry, the ratio stays around unity, indicating that correlation effects are unimportant for all the q values considered here, except for $q=0.1$ a.u. where correlations are very significant up to 120 Ry. Interestingly, at low values of ω, the ratio corresponding to $q=1.9$ a.u. is the most sensitive to correlations, while for large ω values, greater than about 70 Ry, the ratio for the $q=0.1$ a.u. curve is the most influenced by correlations. The ratio $\eta_{5s\to\epsilon s}(\omega,q)$, not shown, varies within much narrower bounds, $0.3<\eta_{5s\to\epsilon s}(\omega,q)\leqslant 1.5$, in comparison with those of the $5p\to\epsilon p$ transition.

Figure 4(b) depicts the ratio $\eta_{4d\to\epsilon d}(\omega,q)$, showing that correlations in the $4d\to\epsilon d$ transition of Xe are much stronger than the correlations in the $3d\to\epsilon d$ transition of Kr and their significance is over the entire range of the ω and q values considered here.

2. Xe dipole channel

The GOS's for dipole transitions in Xe, just as in the same transition of the other noble gases, are characterized by two sets of maxima, but this time they are much closer together and to the ionization threshold, demonstrating the strong influence of the large charge in Xe. A maximum first appears for $q=0.7$ a.u. at $\omega_{\max}\cong 1.3$ Ry and moves forward to $\omega_{\max}\cong 3.8$ Ry, while at the same time decreasing in magnitude, as q increases to $q=1.9$ a.u. For the second set of maxima, reflecting the influence of the Giant Resonance in the $4d\to\epsilon f$ transition, the first maximum corresponding to $q=0.1$ a.u. appears at $\omega_{\max}\cong 7$ Ry and its position moves forward while decreasing in magnitude at the same time, reaching $\omega_{\max}\cong 8$ Ry when $q=1.9$ a.u. For the second set of maxima, the $q=0.1$ a.u. curve corresponds to the largest maximum, while that for $q=1.9$ a.u. represents the smallest maximum.

The role of RPAE correlations is sufficiently large so that the ratio $\eta_{5p\to\epsilon d,s}(\omega,q)$ for values of $\omega<20$ Ry reaches the value 10.3 for $q=0.1$ a.u. For $\omega>20$ Ry the ratio $\eta_{5p\to\epsilon p}(\omega,q)$ is close to unity. Very interesting is the behavior of the ratio $\eta_{5s\to\epsilon p}(\omega,q)$ which is presented in Fig. 4(c). The role of correlations in general and of the giant resonance in the $4d\to\epsilon f$ transition in particular, is very significant. It should be noted that with the growth of q, the primary curve for the $\eta_{5p\to\epsilon p}(\omega,q)$ ratio corresponding to $q=0.1$ a.u. essentially reproduces itself, but on a larger scale, resembling in shape the well-known Xe $5s$ photoionization cross section [54]. The ratio $\eta_{5p\to\epsilon p}(\omega,q)$ first increases with the growth of q, reaching a very large maximum when $q=1.5$ a.u. before decreasing to about 25 when $q=1.9$ a.u. To understand this behavior it is important to bear in mind that the $5s$ photoionization cross section in Xe, just as in Kr $4s$ and even in Ar $3s$, are strongly suppressed, as compared to the cross sections of their np neighbors [54]. Clearly, as q increases, the cross sections are liberated from this suppression.

In Xe the $q=1.5$ a.u. maximum in the ratio $\eta_{5p\to\epsilon p}(\omega,q)$ originally at $\omega_{\max}\cong 9.5$ Ry in the first set of maxima, moves to $\omega_{\max}\cong 13.6$ Ry in the second set. Beyond about 25 Ry correlations become insignificant right up to 120 Ry. Figure 4(d) depicts the variation of the ratio $\eta_{4d\to\epsilon f,p}(\omega,q)$, which shows that correlations in the $4d\to\epsilon f,p$ transitions in Xe are much stronger than those in the $3d\to\epsilon f,p$ transition in Kr. Strong oscillations, varying between 0.47 and 1.37, characterize the ratio $\eta_{4d\to\epsilon f,p}(\omega,q)$ in the energy region $\omega<30$ Ry. For $\omega>30$ Ry this ratio approaches monotonically unity for all the q values considered here, except that correlations influence the $q=1.9$ a.u. ratio less when compared with that belonging to the others. Note that for the first set of maxima the ratio $\eta_{4d\to\epsilon f,p}(\omega,q)$ corresponding to the $q=1.9$ a.u. value has the largest maximum, but in the second set of maxima, it has assumed the lowest value compared to the rest of the curves. Also, the position of $q=1.9$ a.u. maximum is shifted to a higher value of ω in comparison with that of the $q=0.1$ a.u. curve.

3. Xe quadrupole channel

As seen from Fig. 4(e) the quadrupole GOS's in Xe are characterized by three sets of prominent maxima for all the q values considered, particularly those corresponding to $q>0.1$ a.u. In the first set, the maxima are rapidly increasing with the growth of q, up to 1.1 a.u. where they reach the absolute maximum value before they start to decrease as q increases beyond 1.1 to 1.9 a.u. The position of the maximum moves from 1.3 Ry when $q=0.1$ a.u. to 2.0 Ry when $q=1.9$ a.u. For the second set of maxima, the maximum corresponding to $q=0.3$ a.u. moves from $\omega_{\max}\cong 2.9$ Ry to $\omega_{\max}\cong 5.7$ Ry for $q=1.9$ a.u. For the third set of maxima,

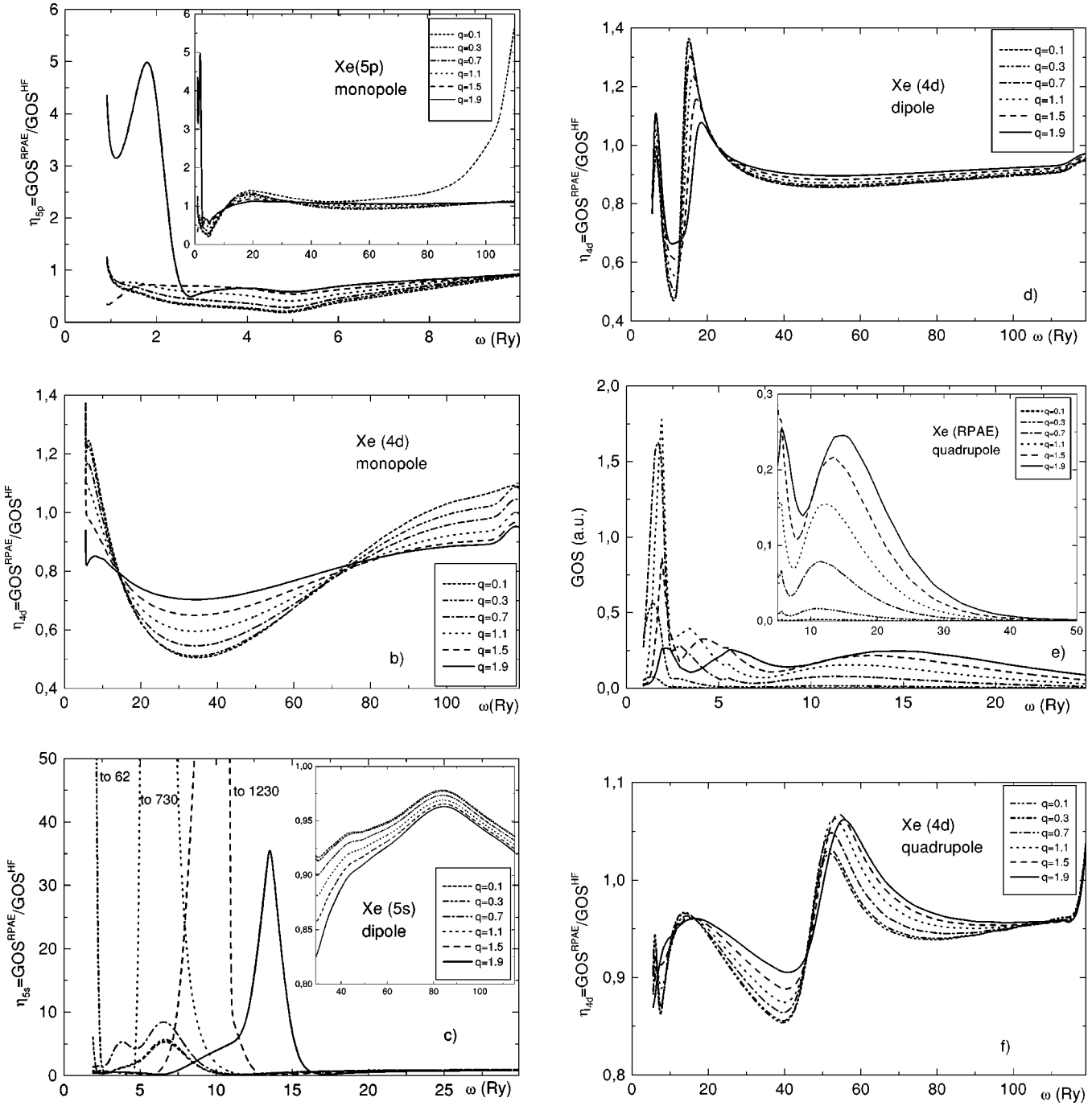

FIG. 4. Generalized Oscillator Strengths for Xe atom as functions of the transferred energy ω (Ry) and momentum q (a.u.). (a) Ratio of *monopole* GOS densities for *5p* electrons, with and without RPAE correlations, $\eta_{5p\to\varepsilon d,s}(\omega,q)\equiv G^{RPAE}_{5p\to\varepsilon d,s}(\omega,q)/G^{HF}_{5p\to\varepsilon d,s}(\omega,q)$. (b) Ratio of *monopole* GOS densities for *4d* electrons, with and without RPAE correlations, $\eta_{4d\to\varepsilon d}(\omega,q)$. (c) The ratio of *dipole* GOS densities for *5s* electrons, with and without RPAE correlations, $\eta_{5s\to\varepsilon p}(\omega,q)$. (d) Ratio of *dipole* GOS densities for *4d* electrons, with and without RPAE correlations, $\eta_{4d\to\varepsilon f,p}(\omega,q)$. (e) *Quadrupole* GOS total density $[G^{RPAE}_{5p\to\varepsilon f,p}(\omega,q)+G^{RPAE}_{5s\to\varepsilon d}(\omega,q)+G^{RPAE}_{4d\to\varepsilon g,d,s}(\omega,q)]$ in RPAE. (f) Ratio of *quadrupole* GOS densities for *4d* electrons, with and without RPAE correlations, $\eta_{4d\to\varepsilon g,s}(\omega,q)$.

the maximum increases monotonically with the growth of q, from $\omega_{\max}\cong 11$ Ry when $q=0.3$ a.u. to $\omega_{\max}\cong 14.8$ Ry for $q=1.9$ a.u.

Figure 4(f) shows the effects of the RPAE correlations represented by the ratio $\eta_{4d\to\epsilon g,s}(\omega,q)$ for the quadrupole transition $4d\to\epsilon g,s$ in Xe. Just as for the $3d\to\epsilon g,s$ in Kr, they are relatively weak in the Xe $4d\to\epsilon g,s$ transition. However, they are represented by a very interesting oscillatory structure, varying between the bounds of about 0.85 and 1.10, right to the highest value of ω considered. Close to 120 Ry, the q-dependence of the correlations disappears, the curves become indistinguishable and approach the $\omega=120$ Ry value with a steep slope. The ratio $\eta_{5p\to\epsilon f,p}(\omega,q)$, varying between the limits of 0.58 and 1.3,

demonstrates essentially the influence of the RPAE correlations upon the $5p$ subshell. The effects of correlations, determined by the ratio $\eta_{5s\to\epsilon d}(\omega,q)$, upon the GOS's of the $5s$ subshell are much stronger than those upon the $5p$ subshell for which the ratio is $\eta_{5p\to\epsilon f,p}(\omega,q)$. The former ratio has for all the q values examined here, a large maximum with its smallest value being 5. For $q=0.7$ a.u. the former ratio reaches a very high value of 3500, which is a result of a zero in the $G^{HF}_{5s\to\epsilon d}(\omega,q)$ at $q=0.1$ a.u. for $3.8<\omega<5.3$ Ry.

IV. SUMMARY AND DISCUSSION OF RESULTS

In this investigation of the GOS's of the noble-gas atoms, we have found that as q increases, the relative role of correlations, particularly of the intershell ones, changes considerably, in some cases even dramatically. The qualitative explanation for this is found in the oscillations of the operator $\exp(i\vec{q}\cdot\vec{r})$ as a function of $\vec{r}$, which affects differently the matrix elements of the transitions from outer, subvalent and inner subshells of the atoms considered. Consequently, the relative role of the second and first terms in Eq. (8) becomes different, thus leading to considerable differences in the GOS's for given ω and q values.

It is appropriate to begin by discussing the familiar and easier to understand dipole GOS's. In Ne and Ar the influence of the outer $2p^6$ and $3p^6$ subshells upon the inner $2s^2$ and $3s^2$ subshells, respectively, determines all the differences between the HF and RPAE values of the GOS's. Clearly, as seen from Fig. 1(b) the RPAE effects on the GOS's of the $2s$-electron in Ne become stronger with the increase of q. However, the situation is different in Ar. From Fig. 2(b), we see that when q increases the main maximum of the ratio $\eta_{3s\to\epsilon p}(\omega,q)$ decreases. Due to the oscillations of $\exp(i\vec{q}\cdot\vec{r})$ when q increases, the RPAE values of the GOS's as a function of ω acquire an additional maximum at $\omega_{\max}\cong 8.5$ Ry, as compared to the behavior of the exponent at small values of q. In the GOS's for the Ne $2p$, the RPAE effects increase with q, but for Ar $3p$ the role of the RPAE correlations on the GOS's even decreases with the growth in q. For Kr and Xe we have a completely different and complicated situation. Indeed, it is seen from Figs. 3(c) and 3(d) that the Kr GOS curve acquires, with the increase of q, an additional, almost symmetric maximum at about 5 Ry. For Xe $5p$ both its maxima, the first near threshold and the second at about 7 Ry, decrease with increase in q. The same applies to the Kr $4s$ and Xe $5s$ GOS's. In the investigated regime of q, $0\leqslant q\leqslant 1.9$ a.u. our calculations have demonstrated that the RPAE effects on the d electrons do not depend too strongly on q [see Fig. 4(d)].

We next consider the monopole GOS's. As already pointed out above, the monopole GOS's, consistent with the general theory, first start by increasing rapidly, as q^2, with the growth of q. After reaching their maxima at $q_{\max,n}\sim 1/r_n$, where r_n is the radius of the ionized subshell, the GOS's start to decrease as q increases to 1.9 a.u. Figures 1(a) and 3(a) show their behavior for Ne and Kr, respectively. The role of RPAE correlations varies considerably with the growth of q as seen from Fig. 2(a). Figure 4(a) shows that RPAE effects on the GOS's increase significantly with q growth for all $\omega<3$ Ry and for much higher values of ω the situation is reversed. However, the RPAE effects on the GOS's of the intermediate $3d$ and $4d$ subshells in Kr and Xe, respectively, are modified rather weakly as q increases.

Some comments on the quadrupole GOS's are also appropriate. Their dependence on q for small q values is the same as that for the monopole GOS's. With an increase in q they begin by first growing rapidly, as q^2, and then, after reaching their maxima at $q_{\max,n}\sim 1/r_n$, where r_n is the ionized subshell radius, they begin to decrease. Figures 1(d) and 2(c) display the results for Ne and Ar, respectively. The same basic argument applies to the q dependence of the GOS's for Kr and Xe [see Fig. 4(e)]. The q variation of the RPAE correlations for d electrons is relatively small, but rather complicated as seen in Figs. 3(f) and 4(f).

In summary, the GOS's for Ne, Ar, Kr, and Xe are strongly affected by the multielectron correlations and their relative role is not decreasing but rather increasing, if not always, as q grows.

V. CONCLUSION

We have demonstrated that the electron correlations, both intra- and inter-subshell, are important in the GOS's of the investigated atoms for all the values of ω and q considered in this paper. We have found that additional maxima and minima of entirely many-electron correlation nature appear not only in dipole but also in monopole and quadrupole GOS's. Of great interest is also the q dependence of the GOS's in the dipole channel. All these predictions are nontrivial and deserve careful experimental verification. Furthermore, we expect that the results of our calculations will stimulate experimental investigations of fast electron inelastic scattering.

Another source of interest in the *ab initio* GOS data presented above comes from recent investigations of their behavior at small q. Indeed, although it is known that as $q\to 0$ the GOS's must converge to the optical oscillator strengths, the direct approach to this limit using experimental data on inelastic scattering is extremely difficult, if not impossible at all [59]. To reach this limit for a given value of ω one must have $p\to\infty$, which is experimentally impossible to accomplish. Consequently, semiphenomenological and analytical continuation using Regge pole methods [40,41] were developed to clarify the proper behavior of the GOS's at small q [59]. However, these investigations have concentrated mainly on the optically allowed atomic transitions in the region of small q. On the other hand, the calculations within the RPAE framework give rather accurate results, at least it was the case for the photoionization process. Thus, it is quite natural to compare the small q behavior of the GOS's obtained using the RPAE with those calculated from Regge pole studies.

Therefore, our continuing investigation involves studying the small q behavior of the GOS's for dipole, monopole, and quadrupole atomic transitions using the RPAE, particularly since it appears that multielectron correlation effects are significant already at small q values. The study is important in

the context of normalizing the measured relative differential cross sections and guiding their reliable measurement in this region where measurements are difficult to carry out.

ACKNOWLEDGMENTS

M.Ya.A. acknowledges the hospitality of the Center for Theoretical Studies of Physical Systems, Clark Atlanta University. M.Ya.A. and L.V.C. are grateful for the financial support of this research by the Center for Theoretical Studies of Physical Systems, Clark Atlanta University. They also acknowledge the financial support of the International Science and Technology Center, Project No. 1358. A.Z.M. and Z.F. are supported by DoE, Division of Chemical Sciences, Office of Basic Energy Sciences, Office of Energy Research and NASA-PACE.

[1] H. A. Bethe, Ann. Phys. (Leipzig) **5**, 325 (1930).
[2] W. F. Miller and R. L. Platzman, Proc. R. Soc. London, Ser. A **70**, 299 (1957).
[3] E. N. Lassettre, A. Skerbele, and M. A. Dillon, J. Chem. Phys. **50**, 1829 (1969).
[4] L. D. Landau and E. M. Lifschitz, *Quantum Mechanics, Non-Relativistic Theory* (Pergamon, Oxford, 1962).
[5] R. A. Bonham, J. Chem. Phys. **12**, 3260 (1962).
[6] M. Inokuti, Rev. Mod. Phys. **43**, 297 (1971).
[7] W. M. Huo, J. Chem. Phys. **60**, 3544 (1974).
[8] L. Vuskovic, L. Maleki, and S. Trajmar, J. Phys. B **17**, 2519 (1984).
[9] B. Marinkovic, V. Pejcev, D. Filipovic, I. Cadez, and L. Vuskovic, J. Phys. B **25**, 5179 (1992).
[10] S. Trajmar, W. Williams, and S. K. Srivastava, J. Phys. B **10**, 3323 (1977).
[11] B. Marinkovic, V. Pejcev, D. Filipovic, I. Cadez, and L. Vuskovic, J. Phys. B **19**, 2189 (1986).
[12] M. Ismail and P. J. O. Teubner, J. Phys. B **28**, 4149 (1995).
[13] Z. Felfli and A. Z. Msezane, J. Phys. B **31**, L165 (1998).
[14] B. Marinkovic, Z. D. Pejcev, R. Panajotovic, D. M. Filipovic, Z. Felfli, and A. Z. Msezane, J. Phys. B **32**, 1949 (1999).
[15] N. Avdonina, Z. Felfli, and A. Z. Msezane, J. Phys. B **32**, 5179 (1999).
[16] R. Muller-Fielder, K. Jung, and H. J. Ehrhardt, J. Phys. B **19**, 1213 (1986).
[17] L. Vuskovic, S. Trajmar, and D. F. Register, J. Phys. B **15**, 2517 (1982).
[18] A. Saenz, W. Weyrich, and P. Froelich, J. Phys. B **29**, 97 (1996).
[19] T. Y. Suzuki, Y. Sakai, B. S. Min, T. Takayanagi, K. Wakiya, H. Suzuki, T. Inaba, and H. Takuma, Phys. Rev. A **43**, 5867 (1991).
[20] T. Ester and J. Kessler, J. Phys. B **27**, 4295 (1994).
[21] T. Y. Suzuki, H. Suzuki, S. Ohtani, B. S. Min, T. Takayanagi, and K. Wakiya, Phys. Rev. A **49**, 4578 (1994).
[22] Zhifan Chen and A. Z. Msezane, J. Phys. B **31**, 1097 (1998).
[23] K. Z. Xu, R. F. Feng, S. L. Wu, Q. Ji, X. J. Zhang, Z. P. Feng Zhong, and Y. Zheng, Phys. Rev. A **53**, 3081 (1996).
[24] K. N. Klump and E. N. Lassettre, J. Chem. Phys. **68**, 357 (1978).
[25] Zhifan Chen and A. Z. Msezane, Can. J. Phys. **74**, 279 (1996).
[26] E. N. Lassettre and M. A. Dillon, J. Chem. Phys. **59**, 4778 (1973).
[27] Zhifan Chen and A. Z. Msezane, J. Phys. B **31**, 4655 (1998).
[28] Zhifan Chen and A. Z. Msezane, J. Mol. Struct.: THEOCHEM **529**, 55 (2000).
[29] X. W. Fan and K. T. Leung, Phys. Rev. A **62**, 062703 (2000).
[30] I. V. Hertel and K. J. Ross, J. Phys. B **1**, 697 (1968).
[31] N. B. Avdonina, Z. Felfli, D. Fursa, and A. Z. Msezane, Phys. Rev. A **62**, 014703 (2000).
[32] I. D. Williams, A. Chutjian, and R. J. Mawhorter, J. Phys. B **19**, 2189 (1986).
[33] C. C. Turci, J. T. Francis, T. Tyliszczak, G. G. de Souza, and A. P. Hitchcock, Phys. Rev. A **52**, 4678 (1995).
[34] V. Karaganov, I. Bray, and P. J. O. Teubner, Phys. Rev. A **59**, 4407 (1999).
[35] X. Guo, D. F. Mathews, G. Mikaelian, M. A. Khakoo, A. Crowe, I. Kanik, S. Trajmar, V. Zeman, K. Bartschat, and C. J. Fontes, J. Phys. B **33**, 1895 (2000).
[36] X. Guo, D. F. Mathews, G. Mikaelian, M. A. Khakoo, A. Crowe, I. Kanik, S. Trajmar, V. Zeman, K. Bartschat, and C. J. Fontes, J. Phys. B **33**, 1921 (2000).
[37] M. A. Khakoo, M. Larsen, B. Paolini, X. Guo, I. Bray, A. Stelbovics, I. Kanik, and S. Trajmar, Phys. Rev. Lett. **82**, 3980 (1999).
[38] M. A. Khakoo, M. Larsen, B. Paolini, X. Guo, I. Bray, A. Stelbovics, I. Kanik, S. Trajmar, and G. K. James, Phys. Rev. A **61**, 012701 (2000).
[39] N. Avdonina, Z. Felfli, and A. Z. Msezane, J. Phys. B **30**, 2591 (1997).
[40] Z. Felfli, A. Z. Msezane, and D. Bessis, Phys. Rev. Lett. **81**, 963 (1998).
[41] A. Haffad, Z. Felfli, A. Z. Msezane, and D. Bessis, Phys. Rev. Lett. **76**, 2456 (1996).
[42] Zhifan Chen, A. Z. Msezane, and M. Ya Amusia, Phys. Rev. A **60**, 5115 (1999).
[43] Zhifan Chen and A. Z. Msezane, Phys. Rev. A **61**, 030703R (2000).
[44] Zhifan Chen and A. Z. Msezane, J. Phys. B **33**, 2135 (2000).
[45] Zhifan Chen and A. Z. Msezane, J. Phys. B **33**, 5397 (2000).
[46] I. Shimamura, J. Phys. Soc. Jpn. **30**, 824 (1971).
[47] P. S. Ganas and A. E. S. Green, Phys. Rev. A **4**, 182 (1971).
[48] K. J. Miller, J. Chem. Phys. **59**, 5639 (1973).
[49] C. E. Bielschowsky, G. G. B. de Souza, C. A. Lucas, and H. M. Boechat Roberty, Phys. Rev. A **38**, 3405 (1988).
[50] T. C. Wong, J. S. Lee, and R. A. Bonham, Phys. Rev. A **11**, 1963 (1975).
[51] G. P. Li, T. Takayanagi, K. Wakiya, and H. Suzuki, Phys. Rev. A **38**, 1240 (1988).
[52] Qi-Cun Shi, Ke-Zun Xu, Zhang-Jin Chen, Hyuck Cho, and Jia-Ming Li, Phys. Rev. A **57**, 4980 (1998).
[53] T. Takayanagi, G. P. Li, K. Wakiya, H. Suzuki, T. Ajiro, T.

Inaba, S. S. Kano, and H. Takuma, Phys. Rev. A **41**, 5948 (1990).
[54] M. Ya. Amusia, *Atomic Photoeffect* (Plenum Press, New York, 1990).
[55] M. Ya. Amusia and L. V. Chernysheva, *Computation of Atomic Processes* (IOP Publishing, Bristol, 1997).
[56] M. Ya. Amusia, N. A. Cherepkov, L. V. Chernysheva, and S. T. Manson, Phys. Rev. A **61**, 020 701 (2000).
[57] M. Ya. Amusia, A. S. Baltenkov, Z. Felfli, and A. Z. Msezane, Phys. Rev. A **59**, R2544 (1999).
[58] M. Ya. Amusia, A. S. Baltenkov, L. V. Chernysheva, Z. Felfli, and A. Z. Msezane, Phys. Rev. A **63**, 052506 (2001).
[59] Z. Felfli, N. Embaye, P. Ozimba, and A. Z. Msezane, Phys. Rev. A **63**, 012709 (2001).